Comparison of the Physiologically Equivalent Proteins Cytochrome c_6 and Plastocyanin on the Basis of Their Electrostatic Potentials. Tryptophan 63 in Cytochrome c_6 May Be Isofunctional with Tyrosine 83 in Plastocyanin†

G. Matthias Ullmann,*,‡ Markus Hauswald,‡,§ Axel Jensen,§ Nenad M. Kostić,|| and Ernst-Walter Knapp‡

Institut für Kristallographie, Freie Universität Berlin, Takustrasse 6, 14195 Berlin, Germany, Pharma Research, Bayer AG, Aprather Weg, 42096 Wuppertal, Germany, and Department of Chemistry, Iowa State University, Ames, Iowa 50011

Received May 27, 1997; Revised Manuscript Received September 23, 1997⊗

ABSTRACT: The blue copper protein plastocyanin and the heme protein cytochrome c_6 differ in composition and in structure but perform the same function in the photosynthetic electron-transport chain. We compare these two proteins on the basis of their electrostatic potentials in order to understand the structural basis of their functional equivalence. In the first approach, we use a monopole−dipole approximation of the electrostatic potentials to superimpose the proteins. The resulting alignment suggests that Tyr51 in cytochrome c_6 corresponds to Tyr83 in plastocyanin. But since Tyr51 is not conserved in all known cytochrome c_6 sequences, a physiological role of this residue is questionable. In a more sophisticated approach, we applied the recently-developed FAME (*f*lexible *a*lignment of *m*olecule *e*nsembles) algorithm, in which molecules are superimposed by optimizing the similarity of their electrostatic potentials with respect to the relative orientation of the molecules. On the basis of the FAME alignments of plastocyanin and cytochrome c_6, we analyze the docking and the electron-transfer reactions of these two proteins with its physiological reaction partner cytochrome *f*. We derive functional analogies for individual amino acids in possible electron-transfer paths in the interprotein redox reactions. We identify two surface patches in cytochrome c_6 that may be involved in electron-transfer paths. The hydrophobic patch with the exposed heme edge in cytochrome c_6 may be equivalent to the hydrophobic patch with His87 in plastocyanin, whereas Trp63 in cytochrome c_6 may be equivalent to Tyr83 in plastocyanin. An aromatic amino acid is present at the position of Trp63 in all known cytochrome c_6 sequences. The electronic coupling between the heme and the copper site on the one side and several potentially important amino acid residues on the other is analyzed by the Pathways method. We have proposed recently that Lys65 of cytochrome *f* and Tyr83 of plastocyanin form a cation−π system, which may be involved in a two-step mechanism of the electron-transfer reaction between these two proteins from higher plants. Now we corroborate this proposal by analyzing available amino acid sequences.

The blue copper protein plastocyanin serves as a soluble electron carrier in plant and cyanobacterial photosynthesis. It accepts an electron from cytochrome *f*, a part of the membrane-bound cytochrome b_6f complex (*1*, *2*), and donates an electron to $P700^+$ of photosystem I (*3*, *4*). In cyanobacteria and some eukaryotic algae, the heme protein cytochrome c_6 can replace plastocyanin under conditions of copper deficiency (*5*). While the electron-transfer reactions of plastocyanin with various partners have been studied extensively in recent years (for review see refs *5*−*7*), only a few studies examined the electron-transfer reactions of cytochrome c_6 (*8*−*10* and references cited therein).

The structure of plastocyanins from various species has been analyzed by X-ray crystallography and NMR spectroscopy (*5*). Recently, the structure of cytochrome c_6 from two species has been determined (*11*−*13*). In the case of *Chlamydomonas reinhardtii*, the structures of plastocyanin (*14*) and cytochrome c_6 (*12*) are known. The two proteins show completely different secondary and tertiary structures. Plastocyanin has a β-barrel fold, while cytochrome c_6 has a mainly α-helical fold. Since, however, cytochrome c_6 can replace plastocyanin in the cell, the two proteins should have similar surface patterns for the recognition of cytochrome *f* and photosystem I. Indeed, both proteins have a hydrophobic and an acidic patch on their surface (*11*, *12*). The acidic patch in plastocyanin consists of two distinct clusters formed by residues 42−44 and residues 59−61, respectively. In some plastocyanins, including *C. reinhardtii* plastocyanin, two additional acidic residues (residues 53 and 85) are located within the acidic patch (*5*). In the case of plastocyanin, the hydrophobic and the acidic patches are implicated in physiological reactions (*5*−*7*). An electron is transferred from the copper site of plastocyanin to $P700^+$ of photosystem I via the hydrophobic patch (*15*). The electron-transfer path from the heme site of cytochrome *f* to the copper site of plastocyanin seems to involve the highly conserved residue Tyr83 (*16*, *17*), which is located in the acidic patch of plastocyanin. Although Tyr83 and His87 have different distances to the copper atom, their electronic couplings to the copper site are approximately equal (*18*−*21*). Alternatively, the acidic patch of plastocyanin may only be involved

† This work was supported by the Deutsche Forschungsgemeinschaft SFB 312, Project D7, and by the National Science Foundation through Grant MCB-9222741. G.M.U. thanks Boehringer Ingelheim Fonds for a fellowship.

* Correponding author. E-mail: ullmann@chemie.fu-berlin.de. Fax: +49-30-838-3464.

‡ Freie Universität Berlin.

§ Bayer AG.

|| Iowa State University.

⊗ Abstract published in *Advance ACS Abstracts,* December 1, 1997.

S0006-2960(97)01241-5 CCC: $14.00

in the docking to the basic patch of cytochrome *f*, and the electron transfer could conceivably occur in a rearranged configuration, via the hydrophobic patch (*11*, *22*−*24*). We suggested recently that Tyr83 interacts with a cationic side chain in cytochrome *f* in a special way to form a cation−π system, which might be involved in the electron-transfer reaction (*24*). In the case of cytochrome c_6, only the hydrophobic patch was suggested to be involved in electron-transfer reactions (*11*, *12*). A second patch on the surface of cytochrome c_6 through which cytochrome c_6 can exchange electrons has not been identified so far.

The similarity of two proteins is usually defined on the basis of their primary, secondary, or tertiary structures. In the case of the two functionally equivalent electron-carrier proteins plastocyanin and cytochrome c_6, these characteristics are completely different; thus traditional techniques for comparison are inapplicable. Since both proteins dock and react with the same physiological partners and since the pairwise association is mainly caused by electrostatic attraction, we compared plastocyanin and cytochrome c_6 on the basis of their electrostatic potentials. We use the Hodgkin index (*25*) based on the electrostatic potentials of the molecules to define the similarity of the molecules in structural alignments. This index has been used so far only for small molecules, but we apply it as a measure of protein similarity and alignment quality. No prior knowledge about identical or homologous sequences, functional correspondences of amino acids, or information about the active sites of the proteins is required in this new approach.

In order to compare cytochrome c_6 with plastocyanin and to identify surface patches in cytochrome c_6 that may be involved in redox reactions, we use a new method, termed FAME (*f*lexible *a*lignment of *m*olecule *e*nsembles), for aligning proteins in a way that maximizes similarities in their electrostatic potentials (*26*). The approach implemented in FAME is based on the common procedure in medicinal and computational chemistry, the active-analogue approach (*27*), where isofunctional but structurally diverse molecules are compared. The alignments obtained with this method help to identify bioequivalent and sterically equivalent parts of drugs—their pharmacophore pattern. It is possible to identify putative bioactive conformations of isofunctional molecules as local maxima on the high-dimensional similarity hypersurface of the Hodgkin index with respect to local translational, rotational, and torsional parameters of each structure. The alignments of cytochrome c_6 and plastocyanin obtained with FAME should allow us to compare common mechanistic properties and bioequivalent features in these structurally diverse proteins. Our use of electrostatic potentials to align two proteins was motivated by the experimental finding that the association of plastocyanin and of cytochrome c_6 with their reaction partners is greatly diminished by an increase in ionic strength. This dependence is evidence for electrostatic attraction (*8*, *9*, *28*, *29*).

We apply the FAME algorithm with fixed molecular conformations and use electrostatic potentials to align plastocyanin and cytochrome c_6. We analyze electron-tunneling paths (*30*) within plastocyanin and cytochrome c_6, and we compare amino acid sequences of these proteins from various species. On the basis of these investigations, we offer answers to the following questions: Which residues of cytochrome c_6 are functionally equivalent to His87 and Tyr83 in plastocyanin? How are these residues electronically coupled to the heme? Are these residues conserved in the known sequences of cytochrome c_6? Which amino acids can form the lower and the upper cluster of the acidic patch in cytochrome c_6? Is Lys65 of cytochrome *f*, the putative partner of Tyr83 in plastocyanin (*24*), conserved in the available sequences of cytochrome *f*? To our knowledge, this is the first study in which methods originally developed to superimpose small molecules such as drugs are applied to pinpoint structurally and functionally important regions on the surface of biological macromolecules.

MATERIALS AND METHODS

Protein Structures. The properties of plastocyanin and cytochrome c_6 are expected to be most similar if these proteins are from the same organism. The only species for which the structures of both proteins are known is *C. reinhardtii* (*12*, *14*). We used the PDB entries 2plt for plastocyanin and 1cyj for cytochrome c_6. To test the ability of the FAME algorithm to superimpose proteins, we used it to align *C. reinhardtii* plastocyanin with poplar plastocyanin (*31*) (PDB entry 1plc; sequence identity with 2plt, 60%) and with *Pseudomonas aeruginosa* azurin (PDB entry 5azu, chain A) (*32*).

For the superposition of electrostatic potentials with the FAME algorithm and for the calculation of dipole vectors, we deleted all water molecules contained in the crystal structure. They may contribute nonspecifically to the overall electrostatic potential, since their position depends often on the crystalline environment. Only one of the two similar rotamers of the disordered residue Arg57 in *C. reinhardtii* plastocyanin, the one marked A in the PDB entry, was used.

In the calculations of electron-transfer path, all crystal waters were considered. Moreover, we added solvent by placing plastocyanin and cytochrome c_6 separately at the center of a water sphere with a diameter of 19 Å and removing all water molecules that come in sterical conflict with the protein or water molecules in the crystal. The energy of the system, created by this procedure, was minimized using the program CHARMM (*33*). The water molecules were free, while the protein structures were fixed during the energy minimization.

Atomic Charges. The charges of most atoms were taken from the CHARMM22 parameters (*33*). Atomic charges for the blue copper site in plastocyanin, calculated by a density functional method, were kindly supplied by Professor E. I. Solomon and have been published previously (*24*). The same charges were assigned to the blue copper site in azurin. Charges of titratable groups are those at pH 7.0, assuming standard pK_a values. Superpositions were done with cupriplastocyanin and ferricytochrome c_6, since these forms interact with ferrocytochrome *f*. The same charges have been used in the FAME algorithm and in the calculations of the dipole moments.

Amino Acid Sequences. Sequences of plastocyanin, cytochrome c_6, and cytochrome *f* were obtained from the SWISS-PROT data bank. Additional sequences of one plastocyanin and one cytochrome *f* have been published recently (*34*). The numbering of amino acids was taken from the sequences of poplar plastocyanin, *C. reinhardtii* cytochrome c_6, and turnip cytochrome *f*. We analyzed 34 sequences of plastocyanin, 23 of cytochrome c_6, and 20 of cytochrome *f*.

Superposition of Centers of Mass, Dipole Vectors, and Hydrophobic Patches. The dipole vector of each protein was

calculated with respect to its center of mass (*35*). All atomic charges and partial charges of the proteins were considered. The origin of the coordinate system was placed on the centers of mass for both proteins, and the dipoles were aligned by rotating one molecule around the normal to the plane defined by the two dipole vectors. Next, one molecule was rotated around the aligned dipole axis to bring the hydrophobic patches of both molecules close to each other. Keeping the dipole vectors aligned, we minimized the distance between the $N_{\epsilon 1}$ atom of His87 in plastocyanin and the inner carbon atom of the vinyl group at heme ring C (atom CAC in the PDB convention) of cytochrome c_6. These atoms lie at the centers of the respective hydrophobic patches.

Matching of Proteins Based on Electrostatic Potentials. Three-dimensional similarity indices are widely used to compare molecules and provide a quantitative measure of the similarity of two molecules (*36*). We use for this purpose the integral-based Hodgkin index H_{ab}^{elec}, defined in eq 1. The

$$H_{ab}^{\mathrm{elec}} = \frac{2\int \phi_a \phi_b \, \mathrm{d}V}{\int {\phi_a}^2 \, \mathrm{d}V + \int {\phi_b}^2 \, \mathrm{d}V} \tag{1}$$

Coulomb potentials ϕ of the structurally-different molecules a and b are integrated over the whole volume. The numerator quantifies the spatial overlap of the electrostatic potentials ϕ, while the denominator normalizes this value. The resulting similarity index falls in the interval between -1 and $+1$. The value $+1$ corresponds to molecules with identical potentials, whereas -1 corresponds to electrostatic complementarity; this means potentials of the same magnitude but opposite sign. The electrostatic potential ϕ at position $\mathbf{r}$ in a medium with the dielectric constant ε is calculated from point charges q_i assigned to each atom i as given by eq 2; $\mathbf{r}_i$ is the positional vector of atom i. The $1/r$

$$\phi(\mathbf{r}) = \sum_{i=1}^{n} \frac{q_i}{\varepsilon |\mathbf{r} - \mathbf{r}_i|} \cong \sum_{i=1}^{n} \frac{q_i}{\varepsilon} \sum_{\mu=1}^{k} G^{\mu}{}_i(\mathbf{r}) \tag{2}$$

$$G_i^{\mu}(\mathbf{r}) = \gamma_{\mu} \exp(-\alpha_{\mu}(\mathbf{r} - \mathbf{r}_i)^2) \tag{3}$$

term of the Coulomb law can be approximated by a spherical Gaussian function (eq 3). This approximation avoids the singularities of the Coulomb terms and makes the computation approximately 100 times faster than those involving grid evaluation (*37*). In general, two Gaussians are sufficient to fit a $1/r$ curve within a range of 12 Å. By applying standard least-squares fitting techniques with a spherical shell weighting function (*38*), we obtained the following parameters: $\alpha_1 = 0.1247$ Å^{-2}, $\alpha_2 = 0.0065$ Å^{-2}, $\gamma_1 = 0.5168$ Å^{-1}, and $\gamma_2 = 0.1958$ Å^{-1}. With these parameters, the Hodgkin index H_{ab}^{elec} accounts for a significant portion of the electrostatic potentials outside the two protein molecules. The series of integrals reduce to spherical Gaussians with modified prefactors and exponents, which depend only on the pairwise interatomic distances between the two proteins, i.e., on the relative orientation of these molecules. The parameters for these Gaussians are easily calculated (*26*). The analytical formula for the Hodgkin index can be evaluated extremely rapidly, and no singularities exist in this approximation. In a homogeneous medium, the Hodgkin index based on the Coulomb electrostatic potential is independent of the dielectric constant, since the dielectric constant cancels out in eq 1.

We started from 100 different random initial orientations of the two proteins and maximized the Hodgkin index (eq 1) with respect to translational and rotational degrees of freedom to ensure to find the highest maximum several times. About 40% of all maximizations ended at the two highest-ranked superpositions. The highest-ranked alignment can be taken to represent the global maximum of the Hodgkin index. The rotations were parametrized in quaternions, as previously done in SEAL (*39*). Quaternions behave correctly if the rotation matrix is identity, while Euler angles are undetermined in this case (*40*). The FAME method involves a highly efficient eigenvector-following algorithm (*41*) for optimizations, which requires analytic first and second derivatives of the function H_{ab}^{elec}. Typically, 15 steps (minimal 8, maximal 28) were needed to converge to a local maximum of this function. If convergence was reached, i.e., if the norm of the gradient became less than 10^{-10}, the maximization was terminated. One maximization took about 0.5 h on a Mips R8000 CPU. Here, we have summarized only the key points of the method that are necessary to reproduce our results. For a detailed description of the FAME method and additional features of the program, see a forthcoming publication (*26*).

Calculation of Electronic Couplings between the Redox Sites and Surface Atoms. The theoretical basis and the algorithm of the Pathways method are described elsewhere (*30, 42*−*47*). Here we briefly explain only the salient features of the method.

The rate constant (k) for a nonadiabatic electron-transfer reaction is proportional to the square of the tunneling matrix element (T_{DA}) between the donor (D) and the acceptor (A) and to the density of vibrational states weighed by their Franck−Condon factors (the exponent). The symbols λ and $\Delta G°$, respectively, stand for the reorganizational energy and Gibbs free energy of the reaction (*48*).

$$k = \frac{2\pi}{\hbar} |T_{\mathrm{DA}}|^2 \frac{1}{\sqrt{4\pi\lambda RT}} \exp\left(-\frac{(\Delta G° + \lambda)^2}{4\lambda RT}\right) \tag{4}$$

An electron-tunneling path is a trace of interacting covalent bonds, hydrogen bonds, and van der Waals contacts (interactions through space) that link the donor with the acceptor. The respective decay parameters for attenuation of electronic coupling via these bonds and contacts are the unitless quantities ϵ_{C}, ϵ_{H}, and ϵ_{S}, defined in eq 5, and are calculated with the standard parameters α, β, and r_{eq}; r is the distance between the interacting atoms. Coupling within aromatic

$$\epsilon = \alpha \exp(-\beta(r - r_{\mathrm{eq}})) \tag{5}$$

rings of heme, histidine, phenylalanine, tyrosine, and tryptophan and within the guanidinium group of arginine was defined in two ways. In one, bonds were treated as usual covalent bonds ($\epsilon = 0.6$). In the other, the enhanced coupling was recognized by neglecting the attenuation ($\epsilon = 1.0$). The tunneling matrix element for a single path (t_{DA}) is proportional to the relative coupling, according to eq 6.

$$t_{\mathrm{DA}} \propto \prod_i \epsilon_{\mathrm{C}}(i) \prod_j \epsilon_{\mathrm{H}}(j) \prod_k \epsilon_{\mathrm{S}}(k) \tag{6}$$

We recognize that electronic coupling via a given path depends on the degree of covalency of the iron−ligand and copper−ligand bonds included in that path. As in our

Table 1: Hodgkin Indices for the Superpositions of *C. reinhardtii* Plastocyanin with *C. reinhardtii* Cytochrome c_6 (c6), Poplar Plastocyanin (pc), and *P. aeruginosa* Azurin (az) Obtained by Three Methods

superposition method	protein	Hodgkin index[a]
FAME	c6	0.85
	pc	0.92
	az	0.56
dipole alignment	c6	0.75
Kabsch algorithm	pc	0.91

[a] Defined in eq 1.

previous study, in which consideration of anisotropic covalency was introduced into the Pathways algorithm (*20*), we scale the relative coupling by coefficients (γ) representing the contributions of the relevant ligands (L) to the redox molecular orbitals of the electron donor (D) and acceptor (A) (*49*, *50*); see eq 7. This scaling is based on the

$$t_{DA} \propto \gamma_{DL}^{2}\gamma_{AL}^{2}\prod_{i}\epsilon(i) \qquad (7)$$

reasonable assumption that the expansion coefficients γ are independent of the relative coupling. The values of γ were 0.68 for Cys84, 0.11 for His37, 0.11 for His87, and 0 for Met92 in plastocyanin (*18*, *20*) and 1.00 for the porphyrin ligand and 0.6 for each axial ligand in cytochrome c_6. For the sake of consistency with previous publications, we used similar symbols, which vary only in indices, for different physical quantities in eqs 3, 5, and 7.

RESULTS AND DISCUSSION

Optimization of the Superposition of the Electrostatic Potential of C. reinhardtii Plastocyanin with the Electrostatic Potentials of Poplar Plastocyanin and of P. aeruginosa Azurin. To test the utility of the FAME algorithm for superimposing proteins, we have applied it to superimpose plastocyanin from *C. reinhardtii* with two other blue copper proteins: with plastocyanin from poplar and with azurin from *P. aeruginosa*. Poplar plastocyanin and *C. reinhardtii* plastocyanin have sequences that are only 60% identical, but they have very similar electrostatic properties. Plastocyanin from poplar and plastocyanin from *C. reinhardtii*, respectively, have charges of −8 and −6 at pH 7 and dipole moments of 330 and 340 D. The orientation of the dipole in the two proteins is the same. Both azurin and plastocyanin have β-barrel folds. Although they belong to the same structural family (*51*), their electrostatic properties are different. The overall charge of azurin at pH 7 is −1.0, and its dipole moment has a magnitude of only 95 D. In spite of their dissimilar electrostatic properties, both azurin and plastocyanin have a hydrophobic patch close to the copper site.

The relative orientation of the two plastocyanins found with the FAME algorithm is very similar to an orientation found with the Kabsch algorithm (*52*), which minimizes the distances between analogous backbone atoms of two proteins. As Table 1 shows, the Hodgkin indices (eq 1) of the superpositions, found with the FAME algorithm (0.92) and with the Kabsch algorithm (0.91), are nearly equal. The best Hodgkin index found for *C. reinhardtii* plastocyanin and *P. aeruginosa* azurin (0.56) is considerably lower than that for the superposition of the two plastocyanins. Although the electrostatic potentials of plastocyanin and azurin are rather different, their hydrophobic patches overlap in the orientation with the highest Hodgkin index. This overlap shows that analogous surface regions can be identified, even when the proteins compared have different overall electrostatics.

These results show that the Hodgkin index is a good measure of the similarity of electrostatic potentials of proteins. The FAME algorithm is an unbiased and meaningful method for aligning two proteins with similar electrostatics and comparable size. The obtained alignment can be used to compare the reactivity of these proteins.

Superposition of Centers of Mass, Dipole Vectors, and Hydrophobic Patches of Plastocyanin and Cytochrome c_6 from C. reinhardtii. If electrostatic interactions dominate the docking of two proteins, their association depends on ionic strength. The resulting dependence of bimolecular protein−protein reactions on ionic strength can be well described by the van Leeuwen theory (*21*, *53*−*55*), in which the electrostatic potential of the proteins is approximated by its monopole and dipole. Inspired by this theory, we used this approximation of the electrostatic potentials of the two proteins to superimpose plastocyanin and cytochrome c_6. Additionally, we brought the hydrophobic patches of plastocyanin and cytochrome c_6 in proximity to each other by rotating one of them around their aligned dipole axes. A similar attempt was made by Frazao *et al.* (*11*). The total charge of cupriplastocyanin and ferricytochrome c_6 from *C. reinhardtii* at pH 7 is −6; their dipole moments have a magnitude of 340 and 175 D, respectively. The Hodgkin index of this alignment is also listed in Table 1, for comparison.

Besides the total charge and the magnitude of the dipole vector, the angle between the dipole vector and the vector from the center of mass of the protein to the reaction site on the protein surface is an important parameter in the van Leeuwen theory (*53*). The angle between the dipole moment and the vector from the center of mass to the C_γ atom of Tyr83 in plastocyanin is small; in *C. reinhardtii* it is 19°. Therefore, we searched for an aromatic residue in cytochrome c_6 lying at a small angle with respect to the dipole moment. We found Tyr51, which lies at an angle of 23° with respect to the dipole moment.

As Figure 1 shows, both Tyr51 in cytochrome c_6 and Tyr83 in plastocyanin are surrounded by negatively charged residues. The residues in these two proteins that may have similar functions in the recognition of the reaction partners are listed in Table 2. Two residues are considered to be isofunctional if the distance of their acidic groups in the superposition is less than 6.5 Å. Aligned peptide−bond dipoles in α-helices create a macrodipole (*56*) that can have a strong influence on the electrostatics of proteins. The dipole moment arising from the α-helix between residues 33 and 39 in cytochrome c_6 enhances the negative electrostatic potential at the position of residue 41.

The electronic coupling of Tyr51 to the heme is maintained by the sequential neighbor Gln52, which is in van der Waals contact with the heme ring. As Table 3 shows, however, Tyr51 is coupled weakly to the heme. The residue Gln52 is present in all known cytochrome c_6 sequences, but Tyr51 is missing in 10 sequences out of 23 and is replaced by nonaromatic amino acids; see Supporting Information, Figure S1. Only one of the organisms lacking Tyr51 in cytochrome c_6 is a eukaryote. This sequence has been determined by

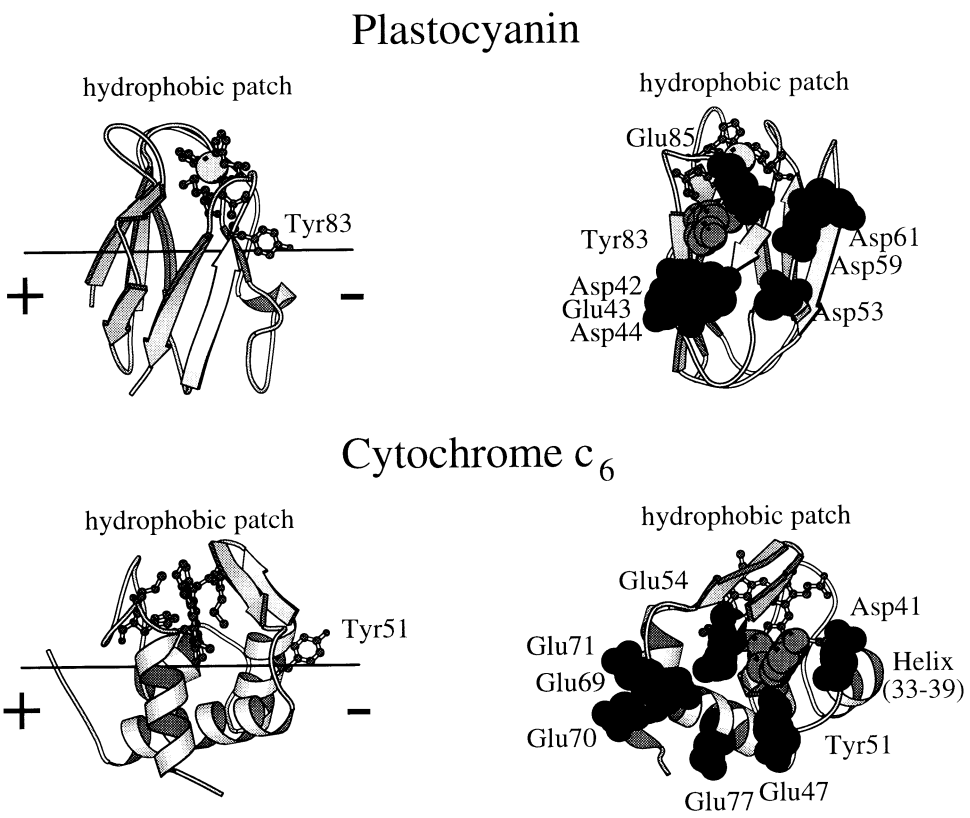

FIGURE 1: Superposition of plastocyanin and cytochrome c_6 from *C. reinhardtii* by alignment of their dipole moments and overlap of their hydrophobic patches. The magnitude of the dipole moment is not proportional to the length of the line. In the left panel, the ligands to the copper atoms and Tyr83 in plastocyanin and also the heme, Cys17, and Tyr51 in cytochrome c_6 are shown as balls and sticks. In the right panel, the protein molecules are rotated by 90° around the vertical axis in the figure plane; the acidic patch points to the viewer. The residues in the acidic patches (dark gray), some of the residues in the hydrophobic patches (ball and stick), and Tyr83 in plastocyanin and Trp83 in cytochrome c_6 (light gray) are highlighted.

Table 2: Corresponding Acidic Residues and α-Helices in Plastocyanin and Cytochrome c_6 from *C. reinhardtii* Identified in Two Superpositions—by Overlaying Centers of Mass, Dipole Vectors, and Hydrophobic Patches and by Optimizing the Match of Electrostatic Potentials

	cytochrome c_6	
plastocyanin	alignment of dipoles	matching of electrostatic fields
Asp42, Glu43, Asp44[a]	Glu69, Glu70, Glu71	Glu70, Glu71
Asp53	Glu47	Glu69
Asp59, Asp61[b]	Asp41, α-helix (33−39)	Glu54, α-helix (46−55)
Glu85	Glu54, α-helix (46−55)	Asp65

[a] Three residues in the lower cluster. [b] Two residues in the upper cluster.

Table 3: Significant Amino Acid Residues on the Protein Surface and Their Properties Relevant to Electron-Transfer Reactions

			squared relative electronic coupling between the residue and the metal site[b]		
protein[c]	residue (electron pair)	distance[a] to the metal site (Å)	$(\Pi\epsilon_i)^2$ $\epsilon_{arom} = 0.6$	$(\Pi\epsilon_i)^2$ $\epsilon_{arom} = 1.0$	$(\Pi\epsilon_i)^2$ $\epsilon_{arom} = 1.0$
plastocyanin	His87 ($C_{\epsilon 2}-H_{\epsilon 2}$)	5	1.7×10^{-2}	4.7×10^{-2}	6.7×10^{-6}
	Tyr83 ($C_\zeta-O_\eta$)	12	4.7×10^{-6}	3.7×10^{-5}	7.7×10^{-6}
cytochrome c_6	Cys17 (S_γ lone pair)	6	3.6×10^{-3}	7.8×10^{-2}	7.8×10^{-2}
	Trp63 ($C_{\eta 2}-C_{\zeta 3}$)	9	9.9×10^{-6}	5.8×10^{-2}	5.8×10^{-2}
	Tyr51 ($C_\zeta-O_\eta$)	15	1.2×10^{-10}	2.6×10^{-8}	2.6×10^{-8}

[a] The distance is measured from the metal atom to the center of the electron pair specified in the second column. [b] Values for different proteins should not be compared because the proportionality factors in eq 6 and 7 may differ. [c] From *C. reinhardtii*.

Edman degradation (57), which is sometimes unreliable. A redetermination of this sequence by a different method would be of interest. All the other cytochrome c_6 sequences lacking Tyr51 are prokaryotic proteins. These facts can be explained in two ways. Either Tyr51 is not involved in the electron-transfer reaction or eukaryotic cytochromes c_6 do use Tyr51 in the electron-transfer reaction whereas prokaryotic cytochromes c_6 do not. The second interpretation, requiring different mechanisms for different species, seems unlikely to us.

Optimization of the Superposition of the Electrostatic Potentials of Plastocyanin and Cytochrome c_6 from C.

reinhardtii. In a second approach, we aligned plastocyanin and cytochrome c_6 using a detailed representation of their electrostatic potentials and optimized the Hodgkin index for the alignment. Each of the 100 optimizations started from a different initial orientation. This search yielded 10 different local maxima, which represent relative orientations of the proteins in which their electrostatic potentials are best matched. The two best superpositions, those with the highest Hodgkin index, differ only very little from each other; 41 out of 100 maximizations ended in one of these two maxima. The hydrophobic patches, for which a functional role has been suggested (*11*, *12*), are superimposed only in these two alignments. Only a few optimizations converged to each of the remaining eight overlays, which correspond to lower Hodgkin indices. In some of these overlays, only the acidic patches overlap, while the remainder of the proteins do not. In other overlays, the hydrophobic patches are on opposite sides; these cases are uninterpretable. In the best superposition, in which the electrostatic potentials are maximally matched, functionally-equivalent residues are expected to be superimposed. For that reason, we discuss only the orientation that has the highest Hodgkin index (0.85; see Table 1). This orientation is shown in Figure 2, in which we compare the electrostatic potentials, the secondary and tertiary structures, and the coupling of the surface atoms to the redox sites of the two proteins.

The similarity of the values 0.85 and 0.92 in Table 1 indicates a high degree of similarity between the electrostatic potentials of plastocyanin and cytochrome c_6. The copper ligand His87 in plastocyanin lies only 3.5 Å away from Cys17 in cytochrome c_6, which is covalently attached to the heme (an iron ligand). Both residues sit in the center of the hydrophobic patches in their respective proteins. Since this patch in plastocyanin is implicated in the electron transfer to photosystem I (*15*), a similar role can be assigned to Cys17 in cytochrome c_6. A similar assignment has already been suggested (*11*, *12*). The residue Tyr83 in plastocyanin is implicated in the electron transfer from cytochrome *f* to plastocyanin (*16*, *17*). The aromatic residue in cytochrome c_6 that sits closest to Tyr83 in the superposition is Trp63. The distance between the centers of aromatic rings of these two amino acids is only 3.5 Å. A rotation of one molecule by a few degrees fully superimposes Cys17 in cytochrome c_6 with the His87 in plastocyanin and also Trp63 in cytochrome c_6 with Tyr83 in plastocyanin. This latter superposition of Trp63 in cytochrome c_6 with Tyr83 in plastocyanin implies similar roles of the two aromatic residues in the electron-transfer reactions of the respective protein with cytochrome *f*. The two residues may be involved in the association with cytochrome *f* or in the subsequent electron-transfer step. An aromatic residue at position 63 can be found in all 23 known sequences of cytochrome c_6. It is tryptophan in 5 and phenylalanine in 18 sequences, as Figure S2 in Supporting Information shows. The replacement of one functionally-important aromatic amino acid by another aromatic amino acid has been observed in several proteins. For example, Tyr83 is replaced by a phenylalanine in two algal plastocyanins, as Figure S3 in Supporting Information shows. The superpositions obtained from the dipole alignment suggested a function for Tyr51 in cytochrome c_6 analogous to that of Tyr83 in plastocyanin. In the superposition with the highest Hodgkin index, the aromatic ring of Tyr51 in cytochrome c_6 is 9.5 Å apart from the center of the aromatic ring of Tyr83 of plastocyanin. This long distance, a sign of non-superimposability of Tyr83 and Tyr51, can be taken as evidence against the involvement of Tyr51 in the electron-transfer reaction between cytochrome c_6 and cytochrome *f*.

Because the aromatic ring of Trp63 is in van der Waals contact with the heme, favorable coupling between them is likely. This and other couplings that may be involved in the interprotein electron-transfer reactions are given in Table 3. As in plastocyanin, where the relative couplings of Cu(II) to His87 and to Tyr83 scaled by the expansion coefficients are comparable, the scaled relative couplings of Fe(II) to Cys17 and to Trp63 in cytochrome c_6 are similar (the last column in Table 3). The relative couplings in plastocyanin and in cytochrome c_6 should not be compared, since the proportionality factors in eq 7 are not necessarily the same for different proteins.

In Figure 3, we compare the positions of acidic residues in plastocyanin and in cytochrome c_6. Two residues are considered analogous to each other if the distance of their acidic groups is less than 6.5 Å. These residues are listed in Table 2. Because an α-helix in cytochrome c_6 between residues 46 and 55 ends near Glu54, the negative end of the dipole moment arising from the α-helix also contributes to the electrostatic potential at Glu54.

Because the pH value within the luminal space of the thylakoids is about 5, we calculated by an established method (*58*) the protonation patterns for plastocyanin and cytochrome c_6 at this pH value. The superpositions found with these protonation patterns do not differ significantly from those obtained with the protonation patterns at pH 7, assuming standard pK_a values (Ullmann and Hauswald, unpublished results). Because there is no clear experimental evidence on which residues have nonstandard protonation in plastocyanin or cytochrome c_6 at pH 5, we describe the results found with protonations at pH 7 assuming standard pK_a's. All conclusions of this study would remain the same if we studied the proteins at the physiological pH value.

A Cation−π System as an Intermediate Electron Acceptor. The electron-transfer reaction between cytochrome *f* and plastocyanin is inhibited by noninvasive cross-linking of these proteins. This finding led to the suggestion that a rearrangement of the initially formed, electrostatic complex is necessary for the electron transfer and that cross-links prevent this rearrangement (*22*). Indeed, rearrangement processes are important in electron-transfer reactions of various protein complexes (*59*−*65*). In a recent theoretical study, we proposed a structural model of the rearrangement of the plastocyanin−cytochrome *f* complex, but we gave also an alternative interpretation of the redox inactivity of the cross-linked complex (*24*). We proposed a cation−π interaction between the side chains of Lys65 in cytochrome *f* and Tyr83 in plastocyanin. Such interactions have recently been documented in synthetic host−guest adducts and biochemical complexes (*66*, *67*), but we are not aware of any investigations of the electrochemical properties of such complexes. However, the system composed of the cation over the aromatic ring may serve as an intermediate electron acceptor in the protein complex, since the cation can stabilize an anion radical at the aromatic ring. If so, the electron-transfer reaction could occur in two steps. An electron is first transferred from the ferroheme in cytochrome *f* to the aromatic ring of the cation−π system at the protein−protein

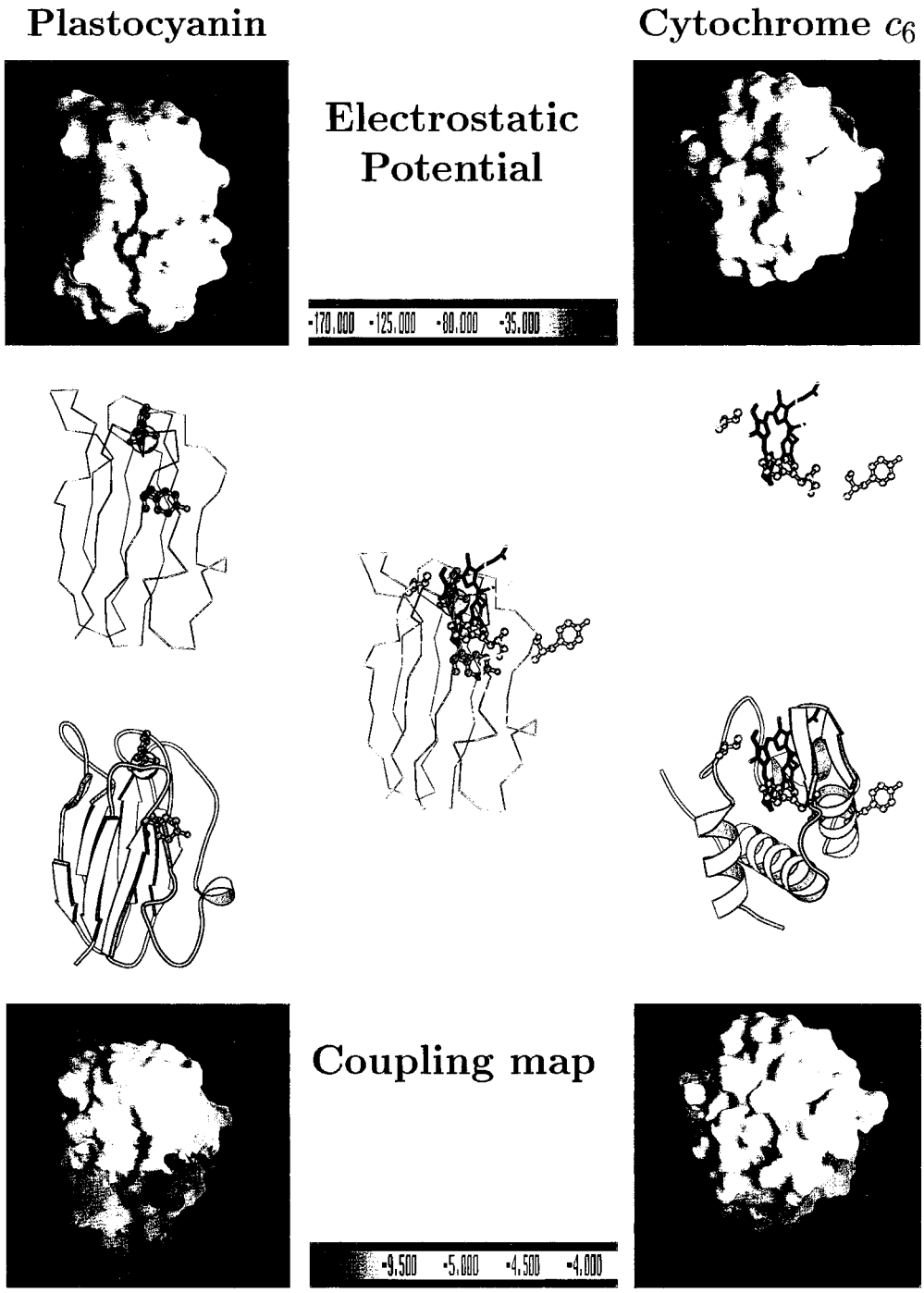

FIGURE 2: Properties of plastocyanin and cytochrome c_6 from *C. reinhardtii* that are relevant to the interprotein electron-transfer reaction. The superposition of the two proteins corresponding to the best match of their electrostatic fields, i.e., the highest Hodgkin index, is shown in the middle of the figure. The separate proteins are kept in the positions so defined. Top part: electrostatic potentials calculated with the uniform dielectric constant of 4. The color is calibrated in units of k_BT, $T = 298$ K. Middle part: C_α traces and secondary and tertiary structures. The copper atom, His87, and Tyr83 in plastocyanin and also the heme, Trp63, Tyr51, and Cys17 in cytochrome c_6 are highlighted. Bottom part: Electronic coupling between surface amino acid residues on the one hand and the iron heme site or the copper site on the other, calculated as in eq 7, taking into account differences in covalency of the various metal−ligand bonds. The decadic logarithm of the square of the relative couplings, $\log((\gamma_{DL}^2 \prod \epsilon_i)^2)$, is mapped onto the molecular surface of the proteins. The strongest coupling is shown in red and the weakest in dark blue.

interface and then from the transient anion radical to the copper site in cupriplastocyanin. The two-step reaction can be faster than the simple one-step reaction if each step is considerably faster than the assumed one-step reaction. The electronic coupling between the heme and the copper site in the plastocyanin−cytochrome *f* complex may be too weak to allow the fast reaction that is observed experimentally.

The redox inactivity of the cross-linked complex can be explained in terms of the two-step mechanism. Cross-linking of Lys65 to an acidic residue disrupts the cation−π interaction between Lys65 and Tyr83. Indeed, residues Glu59 and Glu60 of plastocyanin, which have been implicated in covalent cross-linking between the two proteins (*68*), lie near Lys65 in the calculated configuration of the plastocyanin−cytochrome *f* complex (*24*). Under this hypothesis, the diversion of Lys65 away from Tyr83 would disturb the electron-transfer path and neutralize the cation required for the stabilization of the anion radical of Tyr83.

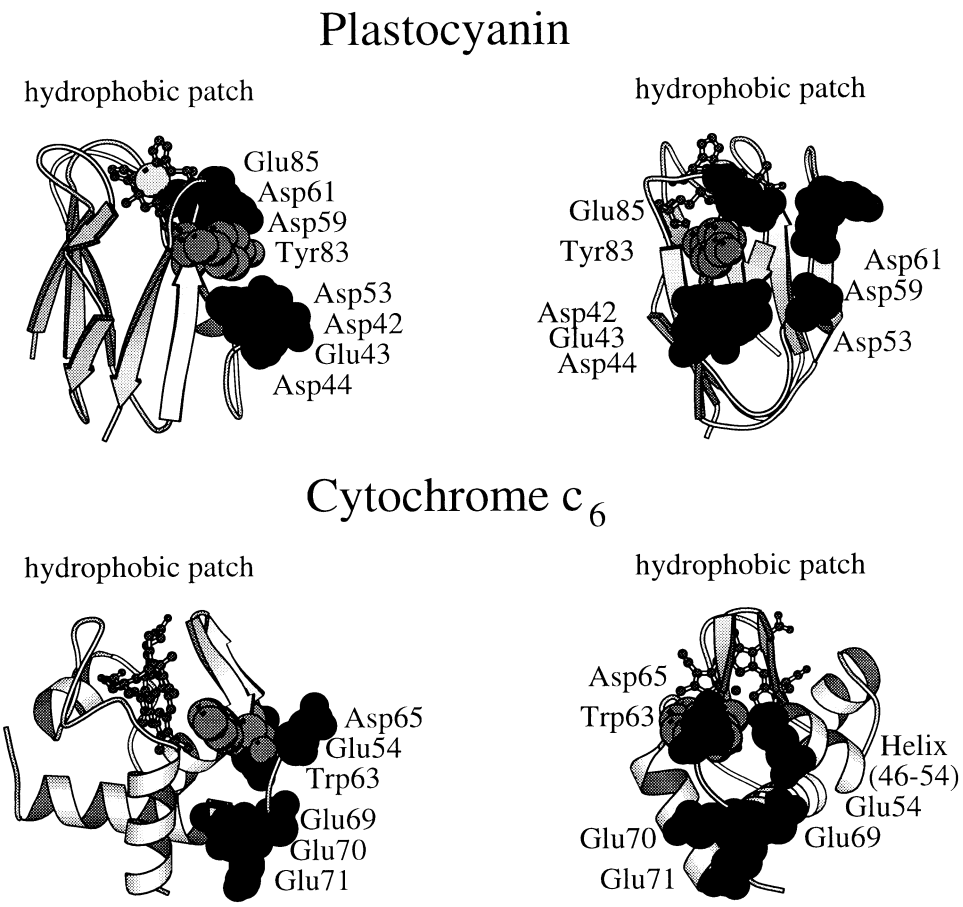

FIGURE 3: Similarity between the acidic patches on the surface of plastocyanin and of cytochrome c_6 from *C. reinhardtii*. The two molecules in the same column adopt the positions corresponding to the best match of their electrostatic fields, i.e., the highest Hodgkin index. On the left side of the figure, the acidic patches point to the right. On the right side of the figure, the protein molecules are rotated by 90° around the vertical axis in the figure plane, so that the acidic patches point to the viewer. The ligands at the metal sites are shown as balls and sticks, acidic residues are in dark gray, and the aromatic residues Tyr83 and Trp63 in plastocyanin and cytochrome c_6, respectively, are in light gray.

The hypothesis of a cation$-\pi$ interaction and of its special role in the electron-transfer mechanism can be tested by analyzing its consistency with the available amino acid sequences. Residue Tyr83 is conserved in nearly all plastocyanins; it is only replaced by a phenylalanine in two algal plastocyanins (Supporting Information, Figure S3). But Lys65 is missing in all cyanobacterial cytochrome *f* sequences and in two eukaryotic algal cytochromes *f* (Supporting Information, Figure S4). These two eukaryotic algae belong to the taxonomic groups *Rhodophyta* (red algae) and *Glaucophyta*, which have rather primitive chloroplasts with many similarities to those in cyanobacteria (*69*). The lack of Lys65 does not necessarily invalidate the proposal that a cation$-\pi$ system serves as a "half-way" electron acceptor in the interprotein reaction. The role of Lys65 may be fulfilled by Lys66, which is conserved in all known cytochrome *f* sequences (Supporting Information, Figure S4).

Lysine side chains are not the only cations potentially capable of interacting with the aromatic π-systems of Tyr83 in plastocyanin. Moreover, both the cation and the aromatic residue may belong to the same protein. The residue at position 88, which is located above the aromatic ring in plastocyanin, is an arginine in all known cyanobacterial plastocyanins (Supporting Information, Figure S4). Their interaction could concievably form a cation$-\pi$ system *within plastocyanin*. This hypothesis is supported by a recent NMR spectroscopic model of a cyanobacterial plastocyanin (*70*). When Lys65 is present in cytochrome *f*, it may interact with Tyr83 in plastocyanin, to form a cation$-\pi$ system at the protein$-$protein interface. When Lys65 is laking in cytochrome *f*, Arg88 and Tyr83 in plastocyanin may form a cation$-\pi$ system within this protein. In either case the interprotein electron-transfer reaction can occur in two steps, because Tyr83 is always involved in a cation$-\pi$ system. The electron transfer in the cyanobacterial plastocyanin$-$cytochrome *f* complex may go via the serine or the glutamine, which replaces Lys65 in cyanobacterial cytochrome *f*. This serine or glutamine residue is a capable hydrogen-bond partner of Arg88 in cyanobacterial plastocyanin (Supporting Information, Figure S4). We have found no amino acid sequence that disagrees with this expanded version of the hypothesis first presented in our previous study (*24*).

Possible Cation$-\pi$ Interaction within Cytochrome c_6. All but two known amino acid sequences of cytochrome c_6 contain a cationic residue (lysine or arginine) in position 66. The crystal structure (*11*) and the NMR spectoscopic model (*13*) of *Monoraphidium braunii* cytochrome c_6 consistently show the spatial proximity of Arg66 and Trp63, possibly a consequence of a cation$-\pi$ interaction. Although the crystal structure of *C. reinhardtii* cytochrome c_6 (*12*) does not show this close proximity, a small reorientation of the side chain of Arg66 is sufficient to bring the guanidinium cation over the indole ring of Trp63, to a position required for a cation$-\pi$ interaction. Because three-dimensional structures of proteins

determined by both X-ray crystallography and NMR spectroscopy are refined by classical force fields, which normally can not account for cation−π interactions (*71*), minor adjustments in the positions of side chains are justifiable. Unlike Arg88 in plastocyanin, Arg66 in cytochrome c_6 is present even in the species whose cytochrome *f* contains Lys65. In these species, Lys65 in cytochrome *f* is probably not required for an efficient electron transfer from that protein to cytochrome c_6. Another possibility would be that Lys65 in cytochrome *f* replaces Arg66 in cytochrome c_6 in the cation−π system after the formation of the protein complex. In the two species in which the cation at position 66 is missing, the cation−π system can presumably form between Lys65 in cytochrome *f* and Trp63 in cytochrome c_6.

We recognize a possibility of a cation−π interaction between Arg66 and Trp63 *within cytochrome* c_6. The electron-transfer reaction between cytochrome *f* and cytochrome c_6, as well as that between cytochrome *f* and plastocyanin, discussed above, may conceivably occur in two steps with an anion radical as a transient intermediate.

Reconsideration of Two Electron-Transfer Reactions between Cytochrome f and Plastocyanin on the Basis of the Two-Step Model. A cyanobacterial cytochrome *f* seems to react differently with plastocyanins from the same cyanobacterium and from spinach, a higher plant. A recent kinetic study (*34*) showed that the former reaction is fast while the latter is very slow at medium ionic strength. Moreover, the former reaction becomes slower and the latter faster as ionic strength is raised. These observations were qualitatively interpreted in terms of electrostatic screening, since plastocyanin from spinach and plastocyanin from this cyanobacterium bear different charges (*34*).

These findings, however, may also be consistent with the notion discussed above that a two-step mechanism for the electron transfer involving a cation−π system is more favorable than a one-step mechanism. The cation−π interaction is present within cyanobacterial plastocyanin, as discussed above. In this case, the electron-transfer reaction may be relatively fast because of it. A cation−π interaction is unlikely within spinach plastocyanin, because this protein lacks a cationic side chain in the correct position with respect to Tyr83, and is also unlikely between this plastocyanin and cyanobacterial cytochrome *f*, because the latter lacks Lys65. Thus, the electron-transfer reaction in this protein complex may be relatively slow, because it cannot occur stepwise.

The different effects of ionic strength on the rate of the two reactions may also be explicable in terms of our new proposal, but this analysis is rather conjectural. We will postpone it until more experimental facts are available. In the meantime, the explanations both in terms of electrostatic screening (*34*) and in terms of cation−π interactions are worth considering. Quantitative kinetic experiments and a more detailed theoretical analysis of the two intriguing reactions are needed.

CONCLUSIONS

A new theoretical method, which was originally designed to superimpose small molecules in order to analyze their bioactive conformations (*26*), is applied for the first time to biological macromolecules to study structure−function relationships. We have demonstrated that the superposition of two proteins on the basis of their electrostatic potentials can provide meaningful information. The Hodgkin index is a useful criterion for quantifying the similarity of electrostatic potentials of two proteins.

We superimposed the blue copper protein plastocyanin and the heme protein cytochrome c_6, which are redox partners of cytochrome *f* in photosynthesis. The hydrophobic surface patches of plastocyanin and cytochrome c_6 overlap in the superposition having the highest Hodgkin index. This finding corroborates recent proposals (*11*, *12*) that the hydrophobic patches of both proteins play similar roles in the electron-transfer reaction. Moreover, the aromatic residues Tyr83 in plastocyanin and Trp63 in cytochrome c_6 also overlap in the best superposition. Since the former is directly bonded to Cys84, a ligand of the copper atom, and the latter is in van der Waals contact with the heme, the two aromatic residues may play similar roles in electron-transfer reactions. This is the first time that a functional analogy between Tyr83 in plastocyanin and Trp63 in cytochrome c_6 has been suggested. In a recent study, we proposed that Lys65 in cytochrome *f* and Tyr83 in plastocyanin form a cation−π system (*24*). The presence of this putative electron acceptor at the protein−protein interface may allow a two-step electron transfer from the heme to the copper site, perhaps involving an anion radical of Tyr83 as a transient intermediate. This study corroborates and extends the new notion that cation−π interactions may occur in redox proteins and their complexes. These interactions may facilitate long-range electron transfer between metal active sites, even though their electronic coupling is very weak.

By considering all known amino acid sequences and three-dimensional structures of plastocyanin, cytochrome c_6, and cytochrome *f*, we propose various cation−π interactions, which may be signs of coevolution of proteins, that are physiological partners. Because cyanobacterial cytochromes *f* lack Lys65, Tyr83 in those cyanobacterial plastocyanins interacts with Arg88 of the same protein. By analogy, Arg66 and Trp63 in cytochrome c_6 seem to interact. This interaction would be yet another piece of evidence for the functional similarity between Tyr83 in plastocyanin and Trp63 in cytochrome c_6. Hence, they are similar not only in the electrostatic environment but perhaps also in their capacity for interactions with cationic side chains. This study suggests that when a cation−π interaction cannot form *between* the physiological partners, it may form *within* one of the partners and thus still facilitate the interprotein electron transfer.

We do not know of experimental findings that disagree with the theoretical proposals in this study. The validity of these proposals will be tested in new experimental studies.

ACKNOWLEDGMENT

We thank Jeffrey J. Regan for the program Greenpath 0.973. M.H. and A.J. thank Dr. Christian Wünsche (Pharma Research, PH-R-SR, Bayer AG) for his constant interest and support.

SUPPORTING INFORMATION AVAILABLE

Four figures showing parts of the aligned amino acid sequences of plastocyanin, cytochrome c_6, and cytochrome *f* (4 pages). Ordering information is given on any current masthead page.

REFERENCES

1. Cramer, W. A., Martinez, S. E., Furbacher, P. N., Huang, D., and Smith, J. L. (1994) *Curr. Opin. Struct. Biol. 4*, 536−544.

2. Cramer, W. A., Soriano, G. M., Ponomarev, M., Huang, D., Zhang, H., Martinez, S. E., and Smith, J. L. (1996) *Annu. Rev. Plant Physiol. Plant Mol. Biol. 47*, 477−508.
3. Fromme, P. (1996) *Curr. Opin. Struct. Biol. 6*, 473−484.
4. Krauss, N., Schubert, W.-D., Klukas, O., Fromme, P., Witt, H. T., and Saenger, W. (1996) *Nat. Struct. Biol. 3*, 965−973.
5. Redinbo, M. R., Yeates, T. O., and Merchant, S. (1994) *J. Bioeng. Biomembr. 26*, 49−66.
6. Sykes, A. G. (1991) *Adv. Inorg. Chem. 36*, 377−408.
7. Sykes, A. G. (1991) *Struct. Bonding 75*, 177−244.
8. Hervás, M., Navarro, J. A., Diaz, A., Bottin, H., and de la Rosa, M. A. (1995) *Biochemistry 34*, 11321−11326.
9. Hervás, M., Navarro, J. A., Diaz, A., Bottin, H., and de la Rosa, M. A. (1996) *Biochemistry 35*, 2693−2698.
10. Navarro, J. A., Hervás, M., and de la Rosa, M. A. (1997) *J. Biol. Inorg. Chem. 2*, 11−22.
11. Frazão, C., Soares, C. M., Carrondo, M. A., Pohl, E., Dauter, Z., Wilson, K. S., Hérvas, M., Navarro, J. A., de la Rosa, M. A., and Sheldrick, G. M. (1995) *Structure 3*, 1159−1169.
12. Kerfeld, C. A., Anwar, H. P., Interrante, R., Merchant, S., and Yeates, T. O. (1995) *J. Mol. Biol. 250*, 627−647.
13. Banci, L., Bertini, I., Quacquarini, G., Walter, O., Diaz, A., Hervás, M., and de la Rosa, M. A. (1996) *J. Biol. Inorg. Chem. 1*, 330−340.
14. Redinbo, M. R., Cascio, D., Choukair, M. K., Rice, D., Merchant, S., and Yeates, T. O. (1993) *Biochemistry 32*, 10560−10567.
15. Haehnel, W., Jansen, T., Gause, K., Klösgen, R. B., Stahl, B., Michl, D., Huvermann, B., Karas, M., and Herrmann, R. G. (1994) *EMBO J. 13*, 1028−1038.
16. He, S., Modi, S., Bendall, D. S., and Gray, J. C. (1991) *EMBO J. 10*, 4011−4016.
17. Modi, S., Nordling, M., Lundberg, L. G., Hansson, Ö., and Bendall, D. S. (1992) *Biochim. Biophys. Acta 1102*, 85−90.
18. Lowery, M. D., Guckert, J. A., Gebhard, M. S., and Solomon, E. I. (1993) *J. Am. Chem. Soc. 115*, 3012−3013.
19. Kyritsis, P., Lundberg, L. G., Nordling, M., Vängard, T., Young, S., Tomkinson, N. P., and Sykes, A. G. (1991) *J. Chem. Soc., Chem. Commun. 8*, 1441−1442.
20. Ullmann, G. M., and Kostić, N. M. (1995) *J. Am. Chem. Soc. 117*, 4766−4774.
21. Qin, L., and Kostić, N. M. (1996) *Biochemistry 35*, 3379−3386.
22. Qin, L., and Kostić, N. M. (1993) *Biochemistry 32*, 6073−6080.
23. Pearson, D. C., Gross, E. L., and David, E. (1996) *Biophys. J. 71*, 64−76.
24. Ullmann, G. M., Knapp, E. W., and Kostić, N. M. (1997) *J. Am. Chem. Soc. 119*, 42−52.
25. Hodgkin, E., and Richards, W. (1987) *Int. J. Quant. Chem. Quant. Biol. Symp. 14*, 105−110.
26. Hauswald, M., Knapp, E. W., and Jensen, A. (submitted for publication).
27. Marshall, G. R., Barry, C. D., Bosshard, H. E., Dammkoehler, R. A., and Dunn, D. A. (1979) in *Computer Assisted Drug Design, ACS Symposium* (Olson, E. C., and Christofferson, R. E., Eds.) Vol. 112, pp 205-226, American Chemical Society, Washigton, DC.
28. Qin, L., and Kostić, N. M. (1992) *Biochemistry 31*, 5145−5150.
29. Kannt, A., Young, S., and Bendall, D. S. (1996) *Biochim. Biophys. Acta 1277*, 115−126.
30. Onuchic, J. N., Beratan, D. N., Winkler, J. R., and Gray, H. B. (1992) *Annu. Rev. Biophys. Biomol. Struct. 21*, 349−377.
31. Guss, J. M., Bartunik, H. D., and Freeman, H. C. (1992) *Acta Crystallogr., Sect. B 48*, 790.
32. Nar, H., Messerschmidt, A., Huber, R., van de Kamp, M., and Canters, G. W. (1991) *J. Mol. Biol. 221*, 765−772.
33. Brooks, B. R., Bruccoleri, R. E., Olafson, B. D., States, D. J., Swaminathan, S., and Karplus, M. (1983) *J. Comput. Chem. 4*, 187−217.
34. Wagner, M. J., Packer, J. C. L., and Bendall, D. S. (1996) *Biochim. Biophys. Acta 1276*, 246−252.
35. Koppenol, W. H., and Margoliash, E. (1982) *J. Biol. Chem. 257*, 4426−4437.
36. Good, A. C. (1995) in *Molecular Similarity in Drug Design* (Dean, P. M., Ed.) pp 25−56, Blackie Academic and Professional, Glasgow.
37. Good, A. C., Hodgkin, E. E., and Richards, W. G. (1992) *J. Chem. Inf. Comput. Sci. 32*, 188−191.
38. Shavitt, I. (1962) *Methods Comp. Phys. 2*, 1−45.
39. Kearsley, S. K., and Smith, G. M. (1990) *Tetrahedron Comput. Methodol. 3*, 615−633.
40. Altmann, S. L. (1986) *Rotations, Quaternions, and Double Groups*, Clarendon Press, Oxford.
41. Baker, J. (1992) *J. Comput. Chem. 13*, 240−253.
42. Beratan, D. N., Onuchic, J. N., Betts, J. N., Bowler, B. E., and Gray, H. B. (1990) *J. Am. Chem. Soc. 112*, 7915−7921.
43. Onuchic, J. N., and Beratan, D. N. (1990) *J. Chem. Phys. 92*, 722−733.
44. Beratan, D. N., Betts, J. N., and Onuchic, J. N. (1991) *Science 252*, 1285−1288.
45. Beratan, D. N., Onuchic, J. N., Winkler, J. R., and Gray, H. B. (1992) *Science 258*, 1740−1741.
46. Betts, J. N., Beratan, D. N., and Onuchic, J. N. (1992) *J. Am. Chem. Soc. 114*, 4043−4046.
47. Regan, J. J., Risser, S. M., Beratan, D. N., and Onuchic, J. N. (1993) *J. Phys. Chem. 97*, 13083−13088.
48. Marcus, R. A., and Sutin, N. (1985) *Biochim. Biophys. Acta 811*, 265−322.
49. Newton, M. D. (1988) *J. Phys. Chem. 92*, 3049−3056.
50. Newton, M. D. (1991) *Chem. Rev. 91*, 767−792.
51. Adman, E. T. (1991) *Adv. Protein Chem. 42*, 145−197.
52. Kabsch, W. (1976) *Acta Crystallogr., Sect. A32*, 922−923.
53. van Leeuwen, J. W. (1983) *Biochim. Biophys. Acta 743*, 408−421.
54. Zhou, J. S., and Kostić, N. M. (1992) *Biochemistry 31*, 7543−7550.
55. Zhou, J. S., and Kostić, N. M. (1993) *Biochemistry 32*, 4539−4546.
56. Hol, W. G. J., van Duijnen, P. T., and Berendsen, H. J. C. (1978) *Nature 273*, 443−446.
57. Okamoto, Y., Minami, Y., Matsubrara, H., and Sugimura, Y. (1987) *J. Biochem. (Tokyo) 102*, 1251−1260.
58. Bashford, D., and Karplus, M. (1990) *Biochemistry 29*, 10219−10225.
59. Zhou, J. S., and Kostić, N. M. (1993) *J. Am. Chem. Soc. 115*, 10796−10804.
60. Qin, L., and Kostić, N. M. (1994) *Biochemistry 33*, 12592−12599.
61. Ivković-Jensen, M. M., and Kostić, N. M. (1996) *Biochemistry 35*, 15095−15106.
62. Crnogorac, M. M., Shen, C., Young, S., Hansson, Ö., and Kostić, N. M. (1996) *Biochemistry 35*, 16465−16474.
63. Nocek, J. M., Zhou, J. S., Forest, S. D., Priyadarshy, S., Beratan, D. N., Onuchic, J. N., and Hoffman, B. M. (1996) *Chem. Rev. 96*, 2459−2490.
64. Davidson, V. L. (1996) *Biochemistry 35*, 14036−14039.
65. Ivković-Jensen, M. M., and Kostić, N. M. (1997) *Biochemistry 36*, 8135−8144.
66. Dougherty, D. A. (1996) *Science 271*, 163−168.
67. Ma, J. C., and Dougherty, D. A. (1997) *Chem. Rev. 97*, 1303−1324.
68. Morand, L. Z., Frame, M. K., Colvert, K. K., Johnson, D. A., Krogmann, D. W., and Davis, D. J. (1989) *Biochemistry 28*, 8039−8047; (1989) *Biochemistry 28*, 10093 (Correction).
69. Köhler, S., Delwiche, C. F., Denny, P. W., Tilney, L. G., Webster, P., Wilson, R. J. M., Palmer, J. D., and Ross, D. S. (1997) *Science 275*, 1485−1489.
70. Badsberg, U., Jorgensen, A. M., Gesmar, H., Led, J. J., Hammerstad, J. M., Jespersen, L.-L., and Ulstrup, J. (1996) *Biochemistry 35*, 7021−7031.
71. Caldwell, J. W., and Kollman, P. A. (1995) *J. Am. Chem. Soc. 117*, 4177−4178.

BI971241V